SUPPORTING MATERIAL

*Claire Kaiser, Giselle Seguí-Lines, Jason D'Amaral, Adam S. Ptolemy and Philip Britz-McKibbin**

Department of Chemistry, McMaster University, 1280 Main St. W., Hamilton, ON, Canada, L8S 4M1

*To whom correspondence should be addressed: E-mail: britz@mcmaster.ca

Title of Primary Article:

Electrokinetic Probes for Single-step Screening of Polyol Stereoisomers: The Virtues of Ternary Boronate Ester Complex Formation

EXPERIMENTAL

Chemicals and Reagents. De-ionized water used for buffer and sample preparations was obtained using a Barnstead EASYpure®II LF ultrapure water system (Dubuque, Iowa, USA). Phosphate buffer was prepared using potassium phosphate monobasic purchased from Merck (Darmstadt, Germany). The pH of all run buffer solutions used for CE separations were adjusted by using 1.0 M NaOH. All other analytes and reagents used in this study were purchased from Sigma-Aldrich (St. Louis, Mo. USA). Individual analyte stock solutions of 10 mM were prepared in de-ionized water and diluted prior to analysis by CE.

Apparatus and Conditions. All separations were performed on a P/ACE MDQ CE system equipped with single-channel UV absorbance detector (Beckman-Coulter Inc., Fullerton, CA, USA). Uncoated fused-silica capillaries with 75 μm i.d., 360 μm o.d. and 86 cm length with an effective detector length of 76 cm (Polymicro Technologies, Phoenix, USA) were used. A new capillary was first conditioned by high pressure rinsing for 5 min with 0.1 M NaOH, 5 min in de-ionized water and 10 min in background electrolyte. Every separation was then preceded by a 2 min rinse with 0.1 M NaOH and 3 min rinse with background electrolyte prior to sample injection. Hydrodynamic injection of samples were performed at the capillary inlet using a low pressure (0.5 psi or 3.5 kPa) for 3 s. Separations were thermostated at 25ºC using an applied voltage of 30 kV with detection at 280 nm unless otherwise stated. All separations were performed in phosphate buffer with different concentrations of NPBA, sorbitol and/or $MgCl_2$. UV spectra were acquired using a Carey 50 spectrophotometer (Varian Inc., Palo Alto, CA, USA) at room temperature using 20 μM NPBA under different electrolyte conditions. All data processing and linear/non-linear regression was performed using Igor Pro 5.0 (Wavemetrics Inc., Lake Oswego, OR, USA).

Central Composite Experimental Design. A two level (±1)-three factor (*i.e.,* 2^3) central composite design with six axial (± 1.7) and five central (0) conditions for a total of 19 experiments were performed to systematically optimize polyol resolution. The three experimental factors examined were buffer pH (x_1), capillary phosphate concentration (x_2) and temperature (x_3) over a range of 6.4-7.8, 3-37 mM and 16.5-33.5°C, respectively. Multiple linear regression of the data matrix was performed by Excel (Microsoft Inc., Redmond, WA, USA). All experimental design studies were performed using a 100 μM polyol mixture in the sample with 12 mM NPBA in the background electrolyte in order to acquire sufficient resolution between the two pairs of polyols, namely mannitol-galactitol (2-3) and galactitol-sorbitol (3-4).

NMR Spectroscopy. ^{11}B/ ^{31}P-NMR studies were performed using a Bruker AV600 MHz equipped with 5 mm multinuclear TBI-Z probe in order to assess NPBA-phosphate-polyol interactions in solution. All NMR samples consisted of 27 mM phosphate, pH 6.8 containing 10% D_2O with 15 mM NPBA and/or 3 mM sorbitol. Changes in chemical shift as a function of electrolyte composition were reported as relative chemical shift differences (Δδ) to either free phosphate or free NPBA in de-ionized water. In most cases, a significant upfield chemical shift change ($\Delta\delta < 0$) was observed due to changes in the electronic environment of ^{31}P and ^{11}B nuclei as a result of specific covalent interactions of NPBA with phosphate and/or sorbitol.

Human Urine Analysis. A single-point collection of a morning mid-stream urine sample was provided by a healthy volunteer, which was used within 24 hrs while refrigerated at 4°C. All urine samples were centrifuged for 2 min at 10,000 rpm to remove particulate matter and the supernatant was then diluted 10-fold in de-ionized prior to analysis by DC-CE. Recovery and reproducibility studies were performed by analysis of 100 μM spiked polyols in urine using ten replicate samples (n = 10). Analysis of a simulated urinary profile typical for classic galactosemia was also examined to demonstrate adequate selectivity in the presence of elevated galactitol and galactonic acid that have been previously reported to be associated with this metabolic disorder.

THEORY

pK_a Determination by DC-CE. The pH-dependent μ_{ep}^{A} changes of NPBA as a monoprotic acid in phosphate buffer with the addition of 0 or 5 mM sorbitol allowed for determination of its apparent pK_a by non-linear regression based on eq (1):

$$\mu_{ep}^{A} = \frac{K_a}{K_a + [H^+]} \cdot \mu_{ep,C-/AC-} \quad (1)$$

where, μ_{ep}^{A} is the apparent mobility of NPBA or NPBA-sorbitol complex, whereas $\mu_{ep,C-}$ and $\mu_{ep,AC-}$ represent the mobility of conjugate base forms of NPBA and NPBA-sorbitol complex, respectively. It was determined that a 1.2 pH unit lower pK_a for NPBA was induced upon sorbitol complexation reflected by $pK_a = (7.0 \pm 0.2)$ compared to $pK_a^* = (5.8 \pm 0.4)$ as depicted in **Fig. 1(b)** of the manuscript.

Binding Constant Determination by DC-CE. **Fig. 1S** depicts an overlay of double-reciprocal binding isotherms for polyols based on dynamic 1:1 NPBA-polyol interaction in 27 mM phosphate, pH 6.8 using linear regression based on eq (2):

$$\frac{1}{\mu_{ep}^{A}} = \frac{1}{\mu_{ep,AC} K_b^*} \cdot \frac{1}{[C]} + \frac{1}{\mu_{ep,AC-}} \quad (2)$$

where, μ_{ep}^{A} is the apparent mobility of polyol, K_b^* is the apparent binding constant and $\mu_{ep,AC-}$ represent the mobility of the ternary NPBA-polyol-phosphate complex. It is apparent that the magnitude of binding affinity is inversely related to the slope of the plot, with catechol >> sorbitol >> mannitol > galactitol, which reflects the apparent migration order except for mannitol and galactitol. The relative migration order of the latter two polyols can be explained in terms of the magnitude of $\mu_{ep,AC-}$ for each NPBA-polyol complex, which is related to the reciprocal of the y-intercept. In general, maximum binding affinity was observed at pH 7.1, but it significantly decreased at lower (pH 6.4) and higher (pH 7.8) buffer pH conditions. **Table 1S** summarizes the thermodynamic and electrokinetic parameters impacting polyol resolution by DC-CE under optimum conditions, which also includes catechol. Further studies were performed to systematically optimize buffer conditions to maximize polyol stereoisomer resolution, as well as absorbance response for micromolar detection of urinary polyols by DC-CE.

RESULTS AND DISCUSSION

Central Composite Design for Separation Optimization. Since newborn screening for galactosemia require methods that offer high efficiency resolution of elevated galactitol from other neutral polyol stereoisomers, a central composite design was performed to enhance polyol resolution by DC-CE based on three major experimental factors, namely buffer pH, phosphate concentration and capillary temperature. **Table 2S** summarizes the variables, ranges and conditions used in the central composite experimental design for polyol resolution by DC-CE. A total of 19 experiments were performed over the experimental range while measuring two responses related to the resolution of mannitol-galactitol

and galactitol-sorbitol. **Figure 2S(a)** compares the magnitude of the coefficients for each variable (*i.e.,* single, 2-way, 3-way and quadratic) after multiple linear regression of data matrix, which clearly indicated that buffer pH and phosphate concentration were the most significant factors impacting polyol resolution. **Figure 2S(b)** depicts a correlation plot that demonstrates a good fit of the empirical model by comparison of measured and predicted polyol resolution throughout the experimental domain with normal error distribution. Two empirical equations based on a linear combination of the variable coefficients were then used to generate 3D surface response models for prediction of polyol resolution as depicted in **Figure 3S(a) and (b)**. Surface response models provided clear visualization of optimal conditions to maximize the resolution of both pairs of polyol stereoisomers under a single experimental condition. Two different response curves were measured in this study, which represent the resolution between mannitol-galactitol (2-3) and galactitol-sorbitol (3-4). It is apparent that optimal resolution for each pair of polyol isomer occurs under distinct conditions. For instance, a single maximum resolution condition is predicted for mannitol-galactitol (2-3) at 27 mM phosphate, pH 6.9, whereas two maxima conditions are indicated for galactitol-sorbitol (3-4) at 17 mM phosphate, pH 7.8 and 27 mM phosphate, pH 6.4. Thus, buffer pH was the most significant variable impacting polyol resolution, which does not necessarily relate to operating under pH conditions above the pK_a of the boronic acid. **Figure 3S(c)** depicts an overlay of experimental electropherograms based on the three optimal conditions predicted by the surface response models. The greatest resolution for galactitol-sorbitol (3-4) was achieved at 27 mM phosphate, pH 6.4 as shown in **Figure 3S(c)iii**, however this condition resulted in only partial resolution of mannitol-galactitol (2-3). Similarly, **Figure 3S(b)i** highlights excellent resolution of galactitol-sorbitol (3-4), however mannitol-galactitol (2-3) co-migrate as a single peak when using 17 mM phosphate, pH 7.8. It is important to note that the lower phosphate concentration generates less Joule heating at the higher buffer pH with reduced band broadening, but also decreases the polyol signal response. In contrast, **Figure 3S(c)ii** demonstrates that separation using 27 mM phosphate, pH 6.9 achieves baseline resolution of both mannitol-galactitol (2-3) and galactitol-sorbitol (3-4), although the latter resolution was decreased relative to **Figure 3S(b)iii**. Overall, the optimal electrolyte condition to ensure maximum resolution of both pairs of polyols was determined to be 27 mM phosphate, pH 6.8 at 25°C, which was used for the remaining part of this study.

Role of Phosphate and NPBA in the Direct UV Detection of Polyols. Although the importance of the composition of electrolyte solution on the apparent binding behavior of polyols to boronic acids has been noted by several groups, to the best our knowledge, this is the first report that highlights the benefit of specific electrolytes on the spectral properties of boronic acid probes. **Figure 4S(a)** depicts a series of electropherograms that highlight the direct dependence of polyol signal with increasing

phosphate concentration ranging from 3, 7 and 27 mM. It is important to emphasize that all polyols (100 μM) were undetected at 280 nm when using phosphate concentrations under 2 mM, whereas catechol was detected. In addition, higher phosphate concentration also improved polyol resolution due to the slower electroosmotic flow (EOF) and longer residence time for separation. **Figure 4S(b)** summarizes the phosphate-dependence on the average peak area response for polyols and catechol. Despite being intrinsically responsive at UV 280 nm, the molar absorptivity of catechol in fact was enhanced about eight-fold at higher phosphate concentration. However, the most dramatic effect was with the polyols, where a linear increase in absorbance response was measured from 3-20 mM which peaked near 27 mM phosphate, whereas subsequent higher concentrations did not significantly change its absorbance. The use of other common buffer electrolytes, including carbonate and MES, did not generate a similar UV response for polyols compared to phosphate (data not shown). Since phosphate is itself UV-transparent at 280 nm, phosphate clearly does not function merely as a passive electrolyte for pH control, but also selectively interacts with NPBA to enhance NPBA spectral response upon polyol complexation. These observations are consistent with previous studies regarding the role of phosphate in modifying the apparent acidity of boronic acids, as well as their complexation behavior. The inset of **Figure 4S(b)** demonstrates the effect of increasing phosphate concentration on the spectral properties of the NPBA-sorbitol complex, which resulted in an enhancement in its molar absorptivity at 280 nm ($\Delta\varepsilon$) of 3,200 $M^{-1}cm^{-1}$ from 3 to 27 mM phosphate. Further evidence of direct phosphate association with NPBA was also confirmed by NMR experiments, which qualitatively demonstrated that the electronic environment of both phosphorus and boron undergo significant changes as a result of boronic acid complexation with phosphate and sorbitol. This process was vital for inducing the spectral changes in NPBA required for direct absorbance detection of polyols by DC-CE, which is consistent with the formation of the tetrahedral NPBA-sorbitol-phosphate ternary complex depicted in **Scheme 1** of the manuscript.

NMR Studies of Ternary Complex Formation. Further evidence of direct phosphate association with NPBA was also provided by ^{31}P and ^{11}B-NMR experiments as shown in **Figure 5S**. Overall, significant changes in the chemical shift of both ^{31}P and ^{11}B resonances were observed for phosphate and NPBA solutions relative to their free states. For instance, there was a relative upfield shift ($\Delta\delta$) in the ^{31}P resonance for phosphate (27 mM, pH 6.8) of -0.49 and -0.65 ppm with the addition of 15 mM NPBA and 15 mM NPBA with 3 mM sorbitol, respectively. In contrast, the addition of 3 mM sorbitol alone (without NPBA) did not produce any significant change in phosphate chemical shift (data not shown). Similarly, there was a major relative upfield chemical shift ($\Delta\delta$) in the ^{11}B resonance for NPBA in de-ionized water (no phosphate) of -8.84 and -7.32 ppm with the addition of 27 mM phosphate and 27 mM

phosphate with 3 mM sorbitol, pH 6.8, respectively. In addition, the latter condition generated a new high upfield resonance ($\Delta\delta$) at -22.24 ppm, which is characteristic of the tetrahedral NPBA-sorbitol-phosphate ternary boronate ester complex as depicted in **Scheme 1** of the manuscript. These NMR experiments qualitatively confirm that the electronic environment of both phosphorus and boron undergo significant changes as a result of boronic acid complexation with phosphate and sorbitol as ligands/Lewis bases, which was vital for inducing the apparent UV spectral changes in NPBA required for direct absorbance detection of polyols by DC-CE.

Method Validation. Validation studies for DC-CE were performed using 15 mM NPBA in 27 mM phosphate, pH 6.8 with 1.5mM $MgCl_2$ as the optimum separation condition, which provided the maximum resolution of all three polyol stereoisomers. The addition of 1.5 mM Mg^{2+} in the background electrolyte (data not shown) effectively reduced the EOF while not contributing significantly to Joule heating or altering the selectivity of polyol separation. This provided polyols longer residence time in the capillary for separation with resolution exceeding 3.0 that also included the analysis of galactonate and gluconate that are clinically relevant secondary metabolites present in urine. **Table 3S** summarizes the overall validation parameters in terms of linearity, LOD, accuracy and precision. The detection limit (S/N $\approx$ 3) was determined to be about 20 μM, which provided sufficient sensitivity for diagnosis of galactosemia and related sugar metabolic disorders associated with elevated polyol concentrations ($\approx$ 1 mM). The average recovery (n = 10) of a 100 μM spiked urine sample containing the three neutral polyol stereoisomers was determined to be about 94 %. Method reproducibility (n=10) for urine analysis by DC-CE was also assessed in terms of relative peak area and relative migration time using catechol as the internal standard, which provided good precision as reflected by an average CV of 5.2 and 0.3%, respectively. The major advantage of DC-CE is its high selectivity which permits excellent resolution of polyol stereoisomers without interferences in complex biological samples, while offering low cost, simplicity and convenience since it does not require labor-intensive or time-consuming off-line sample pretreatment steps prior to analysis.

Table 1S. Thermodynamic and electrokinetic parameters influencing polyol separation with NPBA using 27 mM phosphate, pH 6.8 by DC-CE.

Analyte	K_b [*†] (M^{-1})	$\Delta H°$ [‖] (kJ mol^{-1})	$T\Delta S°$ [‖] (kJ mol^{-1})	$\mu_{ep,AC-}$ [†] x 10^{-4} (cm^2/Vs)
1. Mannitol	(497 ± 17)	-(10.4 ± 2.3)	(5.1 ± 2.2)	-(1.68 ± 0.02)
2. Galactitol	(453 ± 13)	-(10.5 ± 2.5)	(4.8 ± 2.4)	-(1.77 ± 0.02)
3. Sorbitol	(1255 ± 46)	-(19.4 ± 2.6)	-(1.6 ± 2.6)	-(1.72 ± 0.01)
4. Catechol	(2760 ± 290)	-(17.0 ± 2.8)	(2.8 ± 2.8)	-(2.05 ± 0.04)

[†] *Parameters determined at 25°C, where the average mobility (n=3) of free 3-NPBA was -(7.36 ± 0.02) x 10^{-5}*
[‖] *Thermodynamic parameters were derived form binding isotherms (n =3) at five different temperatures ranging from 20-40°C*

Table 2S. Experimental variables, ranges and conditions selected in the central composite design[†] for optimization of polyol resolution by DC-CE.

Level	pH	[Phosphate] (mM)	Temperature (°C)
-1.7	6.4	3	16.5
-1	6.7	10	20
0	7.1	20	25
1	7.5	30	30
1.7	7.8	37	33.5

[†] *Experimental design was performed as a single replicate for all conditions except for zero condition which was done (n=5) for a total of 19 experiments*

Table 3S. Method validation for single-step analysis of polyols by DC-CE under optimum separation conditions using 27 mM phosphate, 15 mM NPBA, 1.5 mM $MgCl_2$, pH 6.8.

Validation Parameters	Mannitol	Galactitol	Sorbitol
1. Reproducibility (n = 10)			
Relative Migration Time (CV, %)	0.3	0.3	0.2
Relative Peak Area (CV, %)	3.4	7.4	4.8
2. Calibration Curve[†] *(n = 6)*			
Linearity (R^2)	0.9951	0.9973	0.9933
3. Detection Limit (S/N ≈3)			
LOD (μM)	20	20	20
4. Accuracy[‖] *(n = 10)*			
Recovery in Urine (%)	92	86	104

[†] *Calibration curve range from 50-420 μM performed in triplicate at six different concentrations using relative peak areas to the internal standard catechol*

[‖] *Recovery studies performed by spiking 100 μM polyols in a healthy urine sample using ten replicates*

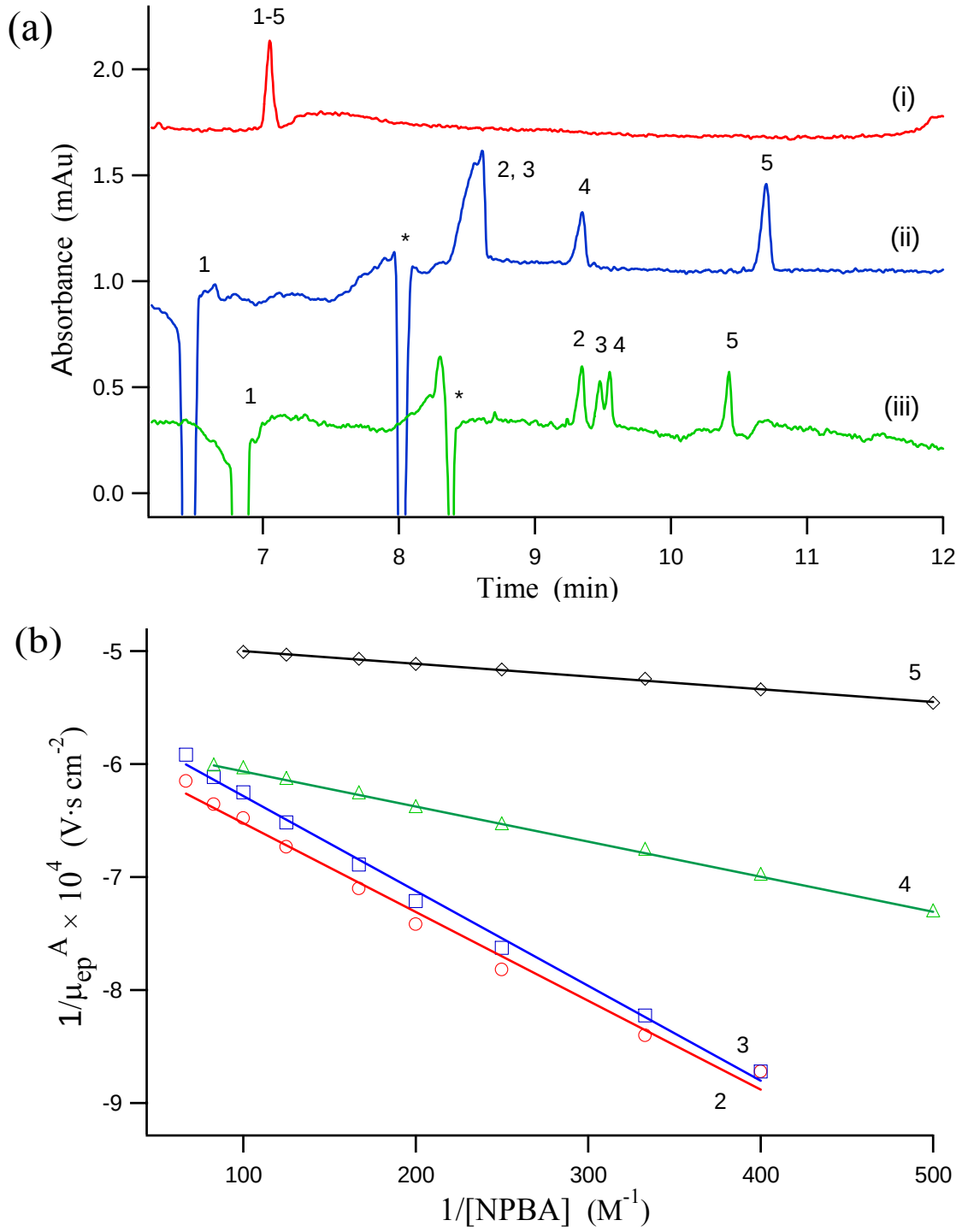

Figure 1S. (a) Electropherograms depicting the impact of increasing NPBA concentration in the background electrolyte for the separation and detection of polyols by DC-CE. Buffer conditions: 20 mM phosphate, pH 7.1 with (i) 0, (ii) 1, (iii) 3 and (iv) 12 mM NPBA. All other operating conditions as described in Fig. 1. (b) Double-reciprocal binding isotherm plots used for determination of thermodynamic and electrokinetic parameters influencing NPBA-polyol separations by DC-CE based on eq (1), where open shapes represent average mobility data (n = 3, CV < 1%) and solid lines represent line of best fit determined by linear regression. Peak numbering in plots correspond to 100 μM of (1) resorcinol, (2) mannitol, (3) galactitol, (4) sorbitol and (5) catechol.

(a)

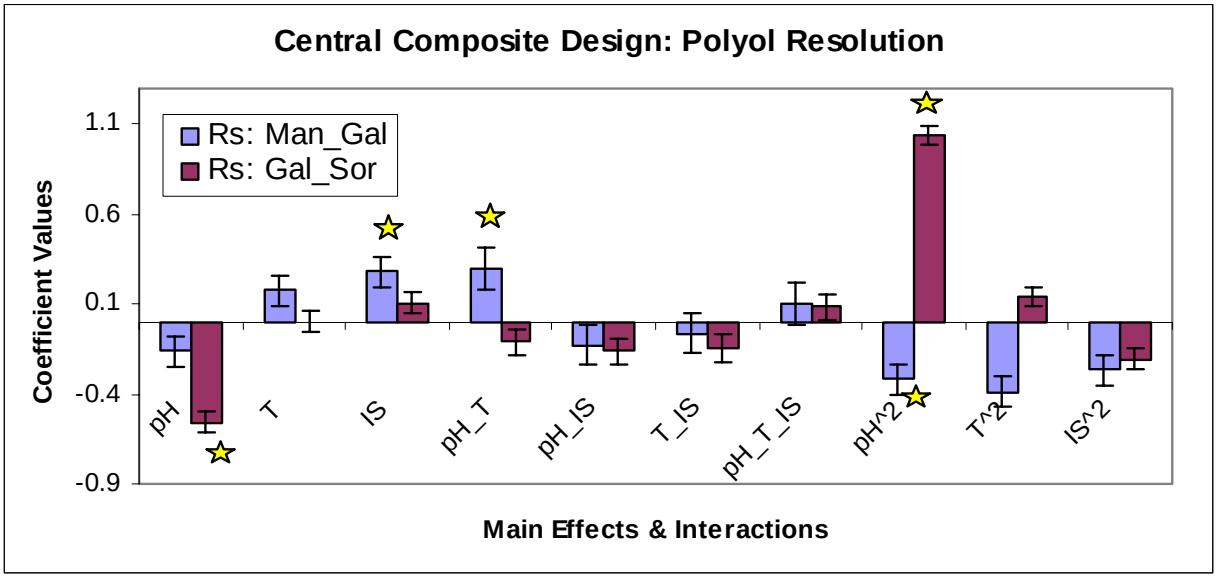

(b)

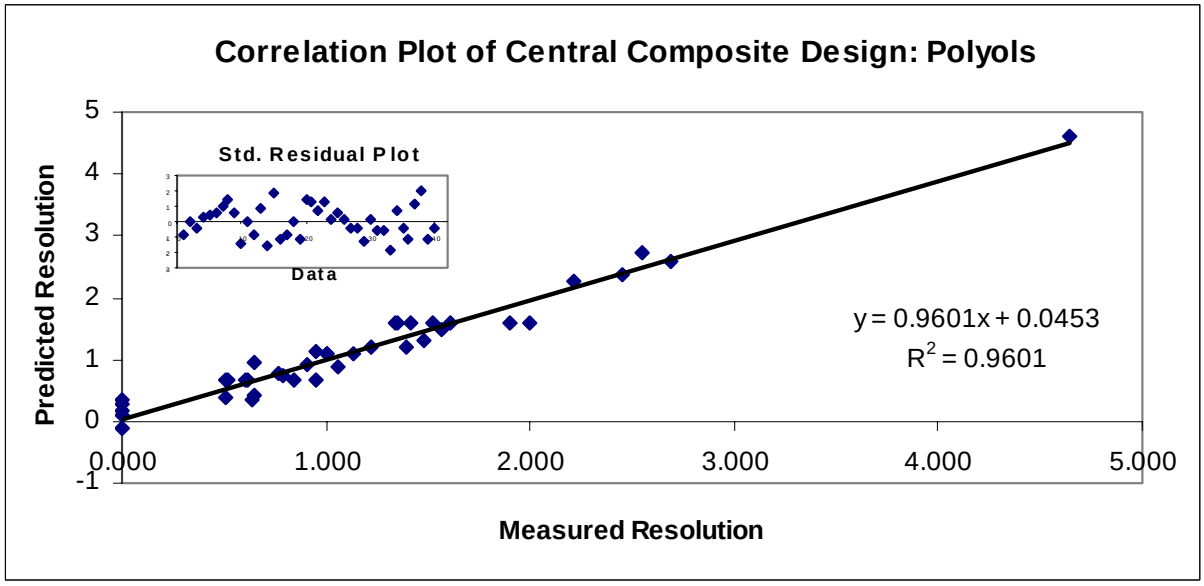

Figure 2S. (a) A summary of single, two-way, three-way and quadratic variables on resolution response for mannitol-galactitol and galactitol-sorbitol using a central composite design model, where stars highlight significant factors at 95% CL. Overall, buffer pH (pH) and phosphate concentration (IS) were the most significant experimental variables unlike column temperature (T). Empirical equations for polyol resolution based on the coefficient terms for the variables were used to construct 3D surface response models. (b) Correlation plot (n=38) of measured and predicted polyol resolution showing good linearity and normal error distribution reflected by the standardized residual plot shown as an inset.

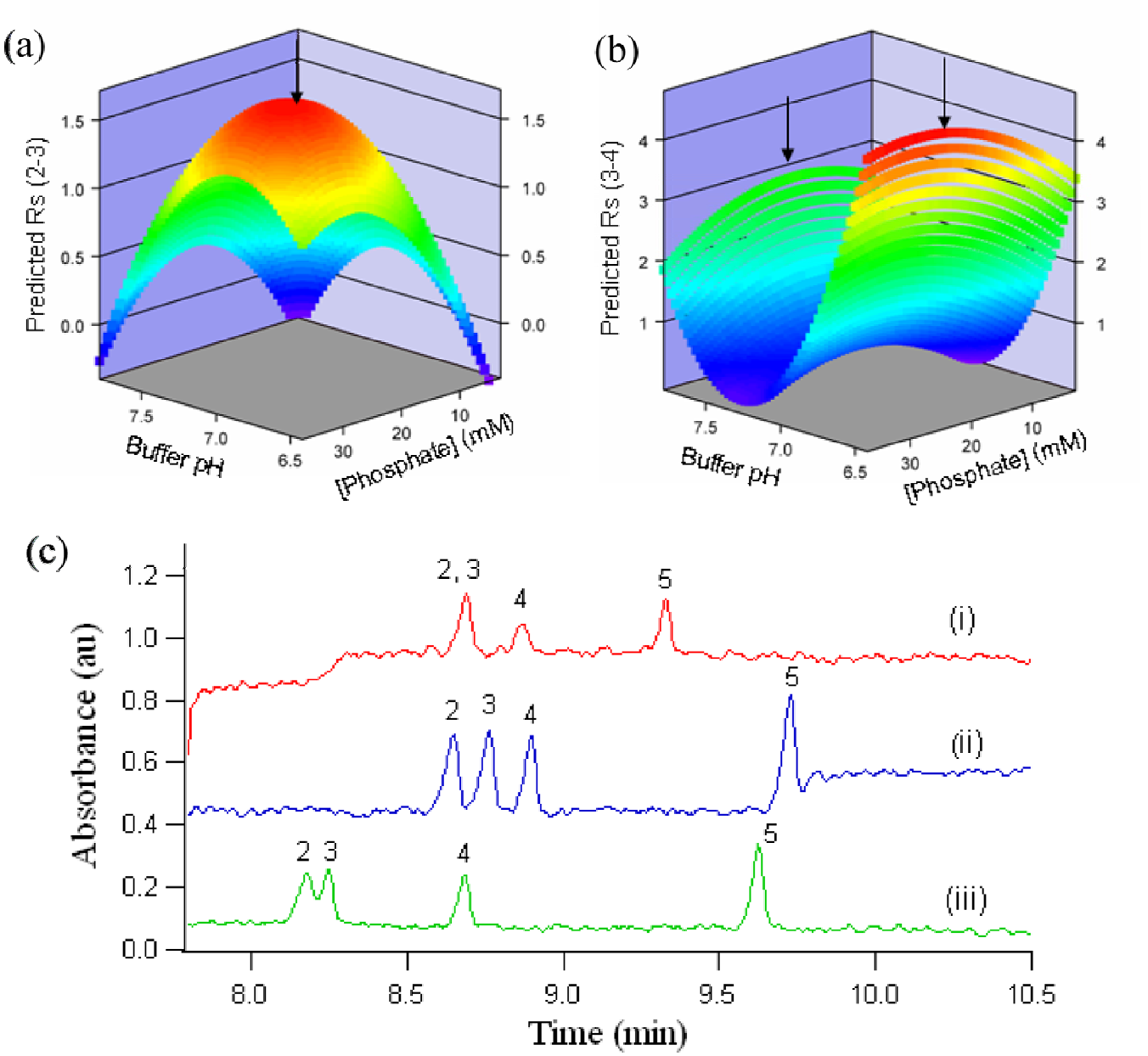

Figure 3S. Surface response models based on a central composite design for the optimization of polyol resolution by DC-CE, namely (a) mannitol-galactitol and (b) galactitol-sorbitol. Three distinct experimental conditions that maximize polyol resolution are indicated by an arrow. (c) Experimental electropherograms for validating optimum conditions predicted by surface response models, where (i) 17 mM phosphate, pH 7.8, (ii) 27 mM phosphate, pH 6.9 and (iii) 27 mM phosphate, pH 6.4.

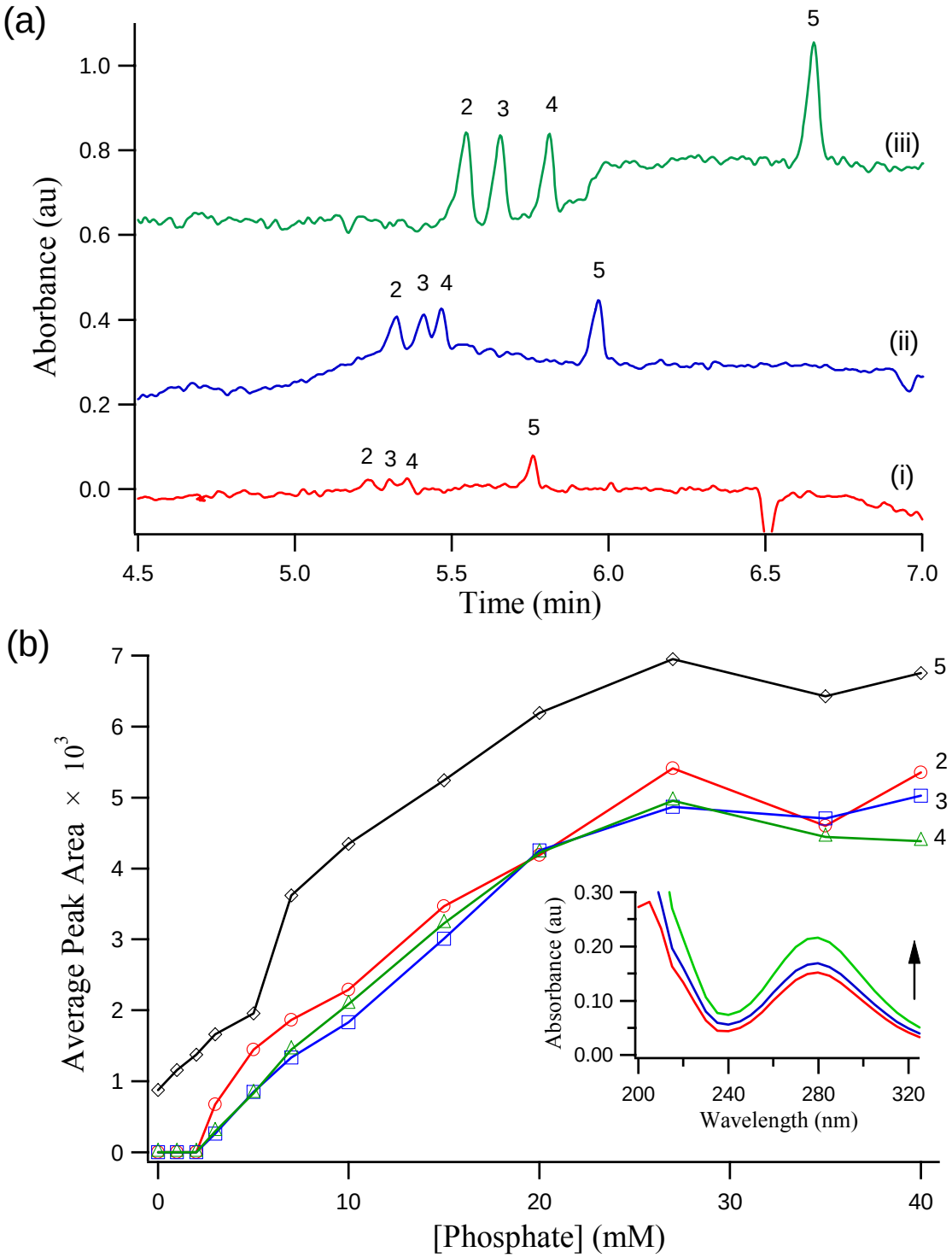

Figure 4S. (a) Electropherograms highlighting the impact of phosphate concentration of the absorbance response for 100 μM polyols at 280 nm using (i) 3, (ii) 7 and (iii) 27 mM phosphate with 15 mM NPBA, pH 6.8. (b) Overall trend depicting dramatic increase in the average peak area (n = 3) for UV-transparent polyols as well as UV-responsive catechol at higher phosphate concentration in the background electrolyte. The inset of (b) shows an overlay of UV spectra for NPBA that confirms the enhancement in molar absorptivity at 280 nm with higher phosphate concentration (3, 7 and 27 mM).

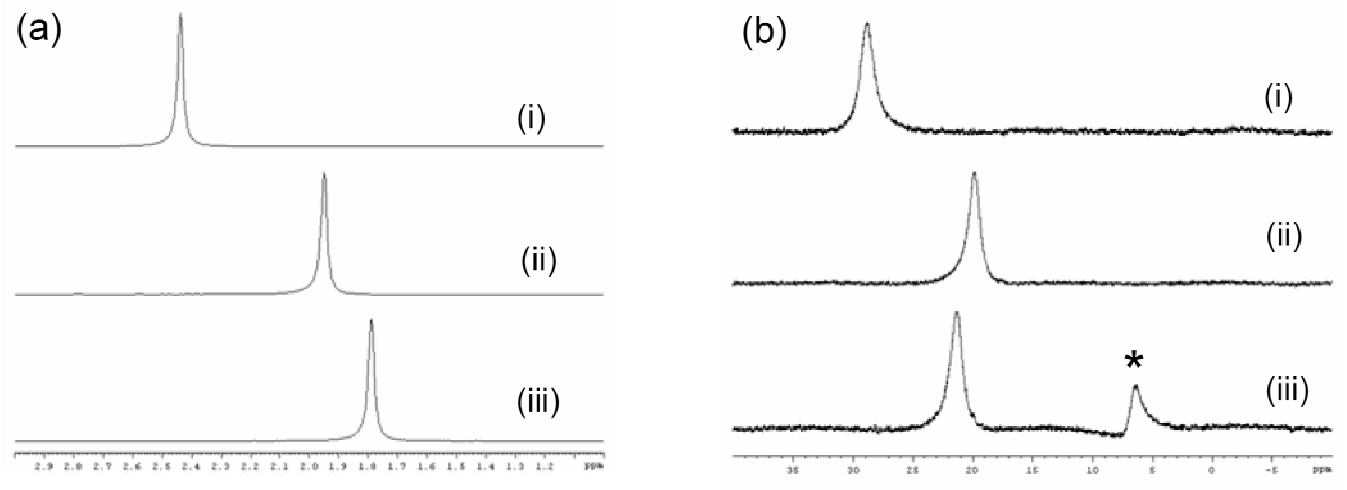

Figure 5S. (a) ^{31}P-NMR spectra showing distinct upfield chemical shift changes for phosphate at pH 6.8 as a function of electrolyte composition, (i) 27 mM phosphate, (ii) 27 mM phosphate, 15 mM NPBA and (iii) 27 mM phosphate, 15 mM NPBA, 3 mM sorbitol. (b) ^{11}B-NMR spectra depicting upfield chemical shift changes for NPBA at pH 6.8 as a function of electrolyte composition, (i) 15 mM NPBA in de-ionized water, (ii) 27 mM phosphate, 15 mM NPBA and (iii) 27 mM phosphate, 15 mM NPBA, 3 mM sorbitol. The extra peak noted by * in (b)(iii) represents the ternary NPBA-sorbitol-phosphate boronate ester complex as depicted in Scheme 1 of the manuscript.